

Hypoxia and Amino Acid Supplementation Synergistically Promote the Osteogenesis of Human Mesenchymal Stem Cells on Silk Protein Scaffolds

Sejuti Sengupta, M.S.,¹ Sang-Hyug Park, Ph.D.,¹ Atur Patel, B.S.,¹ Julia Carn, B.S.,¹
Kyongbum Lee, Ph.D.,² and David L. Kaplan, Ph.D.^{1,2}

Tailoring tissue engineering strategies to match patient- and tissue-specific bone regeneration needs offers to improve clinical outcomes. As a step toward this goal, osteogenic outcomes and metabolic parameters were assessed when varying inputs into the bone formation process. Silk protein scaffolds seeded with human mesenchymal stem cells in osteogenic differentiation media were used to study *in vitro* osteogenesis under varied conditions of amino acid (lysine and proline) concentration and oxygen level. The cells were assessed to probe how the microenvironment impacted metabolic pathways and thus osteogenesis. The most favorable osteogenesis outcomes were found in the presence of low (5%) oxygen combined with high lysine and proline concentrations during *in vitro* cultivation. This same set of culture conditions also showed the highest glucose consumption, lactate synthesis, and certain amino acid consumption rates. On the basis of these results and known pathways, a holistic metabolic model was derived which shows that lysine and proline supplements as well as low (5%) oxygen levels regulate collagen matrix synthesis and thereby rates of osteogenesis. This study establishes early steps toward a foundation for patient- and tissue-specific matches between metabolism, repair site, and tissue engineering approaches toward optimized bone regeneration.

Introduction

INCREASING INCIDENCE OF bone damage due to injury, disease, or tumor resection has given rise to a growing need for bone grafts.^{1–3} Bone regeneration is especially important in cases of critically sized defects where mechanical fixation alone is not sufficient to restore normal bone morphology. The most common treatments, autografts or allografts, are associated with limitations such as donor-site morbidity, risk of infection, and variable graft materials.^{1,3,4} Tissue-engineered bone can provide an alternative method of treatment. The delivery of human mesenchymal stem cells (hMSC) induced to differentiate toward osteoblasts on biodegradable scaffolds has resulted in promising results for bone formation *in vitro* and *in vivo*.⁵ Porous silk scaffolds offer advantages in mechanical strength (average compressive strength = 100 ± 10 kPa, elastic modulus = 1300 ± 40 kPa),⁶ biodegradability, and biocompatibility as a biomaterial platform for regenerating bone.^{6–8} An important issue with any tissue-engineered bone implant is matching the tissue engineering strategy to patient's and implant's site-specific bone regeneration rates to ensure enhanced integration and bone remodeling.^{5,9}

A number of studies have been conducted to tailor biomaterial matrix design to meet specific bone repair needs. In the case of silk biomaterials, significant control over bone morphology can be achieved by altering scaffold design features, for example, stiffness, pore size, interconnectivity between pores, degradability, and processing methods.^{10–14} Computer-aided design and manufacturing and rapid prototyping methods are also being explored to personalize bone implants for specific defect shapes and sizes.¹⁵ In this context of a personalized approach to orthopedic repairs, it is necessary to account for the variability in bone regeneration rates in specific patients (age, sex, genetic make up, and disease state) and defect sites (tissue metabolic activity and bone structure). Local and systemic environmental factors such as cytokines, growth factors, hormones, mechanical stimulus, vascular/nerve factors, and genetic mechanisms play an important role in regulating the osteogenic capacity of an implant.¹⁶ Microenvironmental changes in nutrients, cell density, matrix composition, and matrix functionalization play a role in inducing differentiation of hMSCs.^{17–19} An inter-relationship of stem cell function and metabolism with *in vivo* environmental factors like hypoxia and the absence of glutamine have also

Departments of ¹Biomedical Engineering and ²Chemical and Biological Engineering, School of Engineering, Tufts University, Medford, Massachusetts.

been suggested.^{20,21} However, few attempts have been made to date to identify the influence of hypoxia and amino acid supplements on osteogenesis and metabolism, in a directed manner.

We have reported that the rate of *in vitro* osteogenesis by hMSCs differentiated on silk scaffolds varied depending on how the scaffolds were processed, resulting in different contents of crystallinity and *in vitro* enzymatic degradability.^{6,22} From this recent study, higher osteogenesis rates occurred in more rapidly degrading silk scaffolds than in more slowly degrading scaffolds cultured under the same conditions. This also led to high lysine and proline consumption and a high lactate to glucose ratio.²² On the basis of these results, we hypothesized that lysine and proline supplements and low oxygen levels would increase the rate of osteogenesis.

Amino acids, particularly lysine and proline, are important metabolic factors regulating collagen matrix synthesis during osteogenesis. Collagen type I (Coll) protein constitutes about 90% of the bone extracellular matrix.²³ In addition to providing the framework for structural and functional integrity of bone tissue, Coll regulates the differentiation of osteoprogenitor cells.^{16,24} Optimal collagen deposition is important during bone defect repair.²⁵ Thus, the precursors or building blocks involved in collagen biosynthesis should affect osteogenesis rate. The amino acids proline and lysine constitute important components of the collagen chains and triple helix formation.²⁶ The hydroxylation of these amino acids is critical in the regulation of collagen self-assembly into functional ECM.²⁶ Tsuji *et al.* suggested that the presence of lysine favorably influences osteogenesis of bone marrow cells cultured on hydroxyapatite scaffolds.²⁷ In addition, in our recent study, the osteogenic response by hMSCs differentiated on silk scaffolds with different crystallinity was directly linked to lysine and proline utilization by the cells.²²

Cells are exposed to stringent microenvironmental factors after implantation, such as limited oxygen and nutrient transport, which is likely to alter the viability, differentiation capacity, and functionality of the cells.²⁰ For example, bone fractures usually disrupt the vasculature leading to local tissue hypoxia.²⁸ Consequently, *in vitro* characterization of bone regeneration in the presence of reduced oxygen and understanding the underlying metabolic pathway should aid in rational bone implant designs. However, the effect of hypoxia on bone regeneration still remains debatable. Hypoxia has been reported to stimulate osteogenesis by activating the hypoxia inducible factor (HIF) pathway.^{29–31} Also, as mentioned earlier, higher bone regeneration rates resulted in a higher lactate to glucose ratio, implicating low oxygen in promoting osteogenesis.²² On the other hand, a number of studies have also reported the inhibitory effects of hypoxia on osteogenesis, as evidenced by the downregulation of bone markers, including runt-related transcription factor 2 (*Runx2*), osteocalcin, and Coll.^{32,33} Some enzymes intrinsic to the collagen biosynthetic pathway, for example, prolyl hydroxylase and lysyl oxidase, require molecular oxygen as a substrate. These observations underscore the need to regulate the oxygen concentration within a physiological range when studying *in vitro* osteogenesis systems. Although arterial oxygen tension (pO₂) is 12%, venous, capillary, and interstitial pO₂ is about 5%. The mean pO₂ value of bone marrow aspirates is 6.6%.³³ This suggests that the ambient air conditions used in most *in vitro* bone tissue engineering systems corre-

spond to a state of abnormally high oxygen tension. Thus, in the present study, low (5%) oxygen concentration was studied to conform to the physiological range of oxygen tension.

The current study was aimed at further refining our understanding of the effect of microenvironmental metabolic factors on osteogenic outcomes, with a goal toward predictive models or tools to use in the future to match design to implant site based on a patient's metabolic profile. The variables involved in tissue-engineered bone formation could play a crucial role in osteogenesis outcomes as outlined above and were therefore addressed here. Thus, in the current study, oxygen level and amino acid supplements were assessed, in terms of bone formation *in vitro*. These assessments were also correlated to metabolic profiles, namely, glucose, lactate, and amino acid metabolism. The role of metabolism in osteogenesis is of particular interest, since metabolic processes play an important role in meeting energy and anabolic requirements associated with any regenerative processes, including bone regeneration.³⁴ Bone regeneration rate is directly correlated to cellular metabolic rate.³⁵ Thus, the analysis of metabolic activity inside the cell should help elucidate mechanisms involved in changes in osteogenic responses of the cells in the bone tissue engineering process.

Materials and Methods

Preparation of aqueous-derived silk fibroin scaffolds

Cocoons of *Bombyx mori* were boiled for 30 min in an aqueous solution of 0.02 M Na₂CO₃, and then rinsed thoroughly with distilled water to eliminate the glue-like sericin proteins. The extracted silk fibroin was dissolved in 9.3 M LiBr solution at 60°C for 4 h, yielding a 20% w/v solution. This solution was dialyzed in distilled water using a Slide-a-Lyzer dialysis cassette (MWCO 3500; Pierce) for 2 days. The final concentration of silk fibroin aqueous solution was determined to be 8% w/v. Aqueous-derived silk fibroin scaffolds were prepared by adding 4 g of granular sodium chloride (NaCl; particle size, 500–600 μm) into 2 mL of the silk fibroin solution in cylinder containers. The containers were covered and left at room temperature for 24 h. Then, the containers were immersed in water to extract the salt from the porous scaffolds and the NaCl extracted for 2 days.⁶ The aqueous scaffolds were then cut to our required dimensions (6 mm diameter and 3 mm height) and dried. The aqueous silk scaffolds were sterilized with 70% ethanol.

Three-dimensional in vitro culture of hMSC on aqueous silk scaffolds

hMSC isolation from total bone marrow was carried out as previously reported.³⁶ Cells were then expanded in the hMSC growth medium (Dulbecco's modified Eagle's medium supplemented with 10% fetal bovine serum, 0.1 mM nonessential amino acids, and 1 ng/mL basic fibroblast growth factor in the presence of 100 U/mL penicillin, 100 μg/mL streptomycin, and 0.25 μg/mL fungizone) at 37°C in a 5% CO₂ incubator at 25% oxygen tension. Once sufficient numbers of confluent cells was achieved, passage 3 hMSCs were seeded onto pre-wetted aqueous silk scaffolds (hMSC growth media, overnight) at a density of 1 × 10⁶ cells per scaffold in six-well plates. Two hours after cell seeding, the scaffolds were immersed in their respective osteogenic media. Groups 1 and 3 were dif-

ferentiated in basal osteogenic media containing α -MEM supplemented with 10% fetal bovine serum, 0.1 mM nonessential amino acids, 50 μ g/mL ascorbic acid-2-phosphate, 100 nM dexamethasone, and 10 mM β -glycerolphosphate in the presence of 100 U/mL penicillin, 100 μ g/mL streptomycin, and 0.25 μ g/mL fungizone.¹¹ Groups 2 and 4 were differentiated in lysine- and proline-supplemented media, which contained five times the concentration of lysine and proline than that of basal media. To test the effect of low oxygen conditions on osteogenesis, groups 3 and 4 were maintained at 5% oxygen level incubators (37°C, 5% CO₂), whereas groups 1 and 2 were maintained at 25% oxygen level incubators (37°C, 5% CO₂). Half of the culture medium was replaced and stored for medium analysis every 3 days. The culture medium was changed completely every 2 weeks. The scaffolds were cultured for 7 weeks and samples were removed for analysis at weeks 2 and 7.

Four study groups were used to compare osteogenesis outcomes under the different conditions. Group 1 (control) consisted of hMSCs maintained at 25% oxygen and basal osteogenic medium on ethanol sterilized aqueous silk scaffolds. Group 2 (5 \times lysine and proline) consisted of hMSCs maintained at 25% oxygen but with high lysine and proline concentration medium on the ethanol-sterilized aqueous silk scaffolds. Group 3 (low oxygen) consisted of hMSCs maintained at low (5%) oxygen and basal osteogenic medium (normal content of proline and lysine) on ethanol-sterilized aqueous silk scaffolds. Finally, group 4 (combined effect of low oxygen, 5 \times lysine and proline) had hMSCs maintained at low (5%) oxygen as well as high lysine and proline concentration medium on ethanol-sterilized aqueous silk scaffolds. All the groups consisted of the same hMSC cell source grown and differentiated at the same time to reduce donor differences.

Scanning electron microscopy

The morphology of the different samples was examined at weeks 2 and 7 using scanning electron microscopy (SEM) (Zeiss, FESEM Supra55VP). The samples were fixed for 24 h in formalin, sequentially dehydrated in a series of graded ethanol, and dried before gold coating for 1.5 min before SEM observation.

Histological and immunohistochemical observations

The samples in each scaffold were fixed with 10% neutral buffered formalin and then embedded in paraffin wax and sectioned. The sections were stained with hematoxylin and eosin for histological observation and von Kossa for mineralization. For Coll immunohistochemistry, sections were assessed using the DAB Detection Kit (Ventana Medical Systems, Inc.) according to the manufacturer's instructions. Briefly, sections are digested with endopeptidase to unmask antigen binding sites, exposed to an endogenous peroxidase inhibitor, and incubated with primary Coll antibody (Biodesign) at room temperature. Sections were then incubated with biotinylated IgG and exposed to horseradish peroxidase-labeled streptavidin. Antibody complexes were observed after the addition of a buffered diaminobenzidine solution. The sections were then counterstained in hematoxylin and lithiumcarbonate and mounted. Negative controls are performed similarly in the absence of the primary antibody.¹¹ All

sections were evaluated with a Leica DMIL light microscope and a Leica Application Suite (v3.1.0) software.

Biochemical analysis

For DNA analysis, ($n=3$) samples per group were chopped with microscissors on ice. DNA content was measured using the PicoGreen assay (Molecular Probes), according to the protocol of the manufacturer. Samples were measured fluorometrically at an excitation wavelength of 480 nm and an emission wavelength of 528 nm. The same samples were also tested for alkaline phosphatase (ALP) activity using a biochemical assay (ALPL; Stanbio Laboratory) based on conversion of p-nitrophenyl phosphate to p-nitrophenol, which was measured spectrophotometrically at 405 nm. ALP activity was normalized by DNA content of the sample.

Samples ($n=3$) were extracted with 1 mL 5% (w/v) trichloroacetic acid for total calcium content. Calcium content was determined by a colorimetric assay using orthocresolphthalein complexone (Stanbio Laboratory). The calcium complex was measured spectrophotometrically at 575 nm. In addition, samples ($n=3$) were digested with pepsin (1 mg/mL, pH 3.0) at 4°C overnight for total collagen content. Total collagen of each specimen was measured as following. A dye solution (pH 3.5) was prepared with Sirius red dissolved in picric acid saturated solution (1.3%; Sigma) to a final concentration of 1 mg/mL. The digested samples were dried at 37°C in a 96-well plate for 24 h and then reacted with the dye solution for 1 h on a shaker. After fixing the dye on the sample with fixing solution (15 mL picric acid, 5 mL 35% formaldehyde, and 1 mL glacial acetic acid), the sample was washed three times with 0.01 N HCl and the dye-sample complex resolved in 0.1 N NaOH. The absorbance was read at 550 nm wavelength using an ELISA Reader (Versa MAX; Molecular Devices). The total collagen in each sample was extrapolated using a standard plot of bovine collagen (Sigma) in the range of 0–500 μ g/mL. Both the calcium and collagen content were normalized by dry weight of sample.²²

Semi-quantitative real-time polymerase chain reaction

Fresh samples ($n=3$ per group) were stored in 1.0 mL of Trizol at -80°C . Scaffolds were then chopped with micro scissors on ice and centrifuged at 12,000g for 10 min. About 200 μ L chloroform was added to the supernatant and incubated for 5 min at room temperature. After centrifugation at 12,000g for 15 min, the upper aqueous phase was carefully transferred to a new Eppendorf tube. One volume of 70% ethanol (v/v) was added and applied to an RNeasy mini spin column (Qiagen). The RNA was washed and eluted according to the manufacturer's protocol. The RNA samples were reverse transcribed into cDNA using oligo (dT)-selection according to the manufacturer's protocol (High Capacity cDNA Archive Kit; Applied Biosystems). Transcript levels of *Coll α 1*, *ALP*, *Runx2*, and *HIF-1 α* were quantified using the M 3000 Real-Time PCR system (Stratagene). Polymerase chain reaction conditions were 2 min at 50°C, 10 min at 95°C, and then 50 cycles at 95°C for 15 s, and 1 min at 60°C. The expression data were normalized to the expression of the housekeeping gene, glyceraldehyde-3-phosphate-dehydrogenase, as previously described.⁶ Primer sequences for the human glyceraldehyde-3-phosphate-dehydrogenase gene were as follows: forward

primer 5'-ATGGGGAAGGTGAAGGTCG-3', reverse primer 5'-TAAAAGCCCTGGTGACC-3', and probe 5'-CGC CCAAT ACGACCAAATCCG TTG AC-3'. Primer sequences for the human *Collα1* gene were as follows: forward primer 5'-CAGCCGCTTCACCTACAGC-3', reverse primer 5'-TTTT GTATT CAA TCACTGTCTTGCC-3', and probe 5'-CCG GTGTGACTCGTGCAGCCATC-3'. Primers and probes for *ALP*, *HIF-1α*, and *Runx2* were purchased from Applied Biosciences. Assays-on-Demand™ Gene Expression kits (*ALP*, Product # Hs01029141_g1; *HIF-1α*, Product # Hs00936366_m1; *Runx2*, Product # Hs00298328_s1). Finally, the gene expression level of different groups was expressed in terms of fold increase relative to the gene expression level of the control group.

Media analysis

Aliquots of media ($n = 3$ per study group) were taken every 3 days during media change, stored at -20°C , and later measured for glucose and lactate content in culture media using an ELISA Microtiter plate Reader (Versa MAX; Molecular Devices). Amino acids were also measured by high performance liquid chromatography (Alliance 2690; Waters) (please see details below). The rate of glucose and lactate consumption at weeks 2 and 7 was normalized by DNA content of the scaffolds at the same time point.

Glucose content

Glucose concentration in the medium was determined using glucose oxidase reagent (Pointe Scientific), a modified Trinder's method to develop an efficient peroxidase-phenol-aminophenazone system for the quantitation of hydrogen peroxide by formulation of a red quinoneimine dye.³⁷ The intensity of color produced is directly proportional to glucose

concentration in the sample. For the assay, 200 μL of the glucose reagent was added to 10 μL aliquots of each sample ($n = 3$) or standard (0–1.2 g/L) and incubated at 37°C for 30 min before recording absorbance at 500 nm.

Lactate content

Lactic acid in the medium was measured based on the reduction of nicotinamide adenine dinucleotide to NADH by lactate dehydrogenase. A Lactate Reagent system was used according to the manufacturer's specifications (Trinity Biotech). First, 10 μL of the sample medium was dispensed to wells in triplicate. Next, 200 μL of lactate reagent solution was added (lactate oxidase [400 U/L], peroxidase [2400 U/L], and Chromogen precursor in buffer [pH 7.2]). The absorbance was measured within 30 min using 520–550 nm after incubation at room temperature for 30 min. Values were extrapolated using a lactate standard reference curve in the range of 0–70 mg/dL.

Rates of glucose consumption and lactate production were calculated by the following equation:

$$\text{Rate} = (\text{glucose consumption or lactate synthesis in millimoles} \times \text{media volume}) / (\text{day} \times \text{DNA content in } \mu\text{g})$$

High performance liquid chromatography

Amino acids were quantified by high performance liquid chromatography (Alliance 2690; Waters) using gradient elution and fluorescence-based detection after precolumn derivatization of primary or secondary amines with 6-aminoquinolyl-*N*-hydroxysuccinimidyl-carbamate.^{38,39} Amino acid standards (Pierce) and medium samples were derivatized by AccQ•Fluor Reagent (Waters) according to the manufacturer's instructions. Chromatographic separation was achieved on a Nova-Pak C18 column (4 μm , 3.9 \times 150 mm; Waters) and

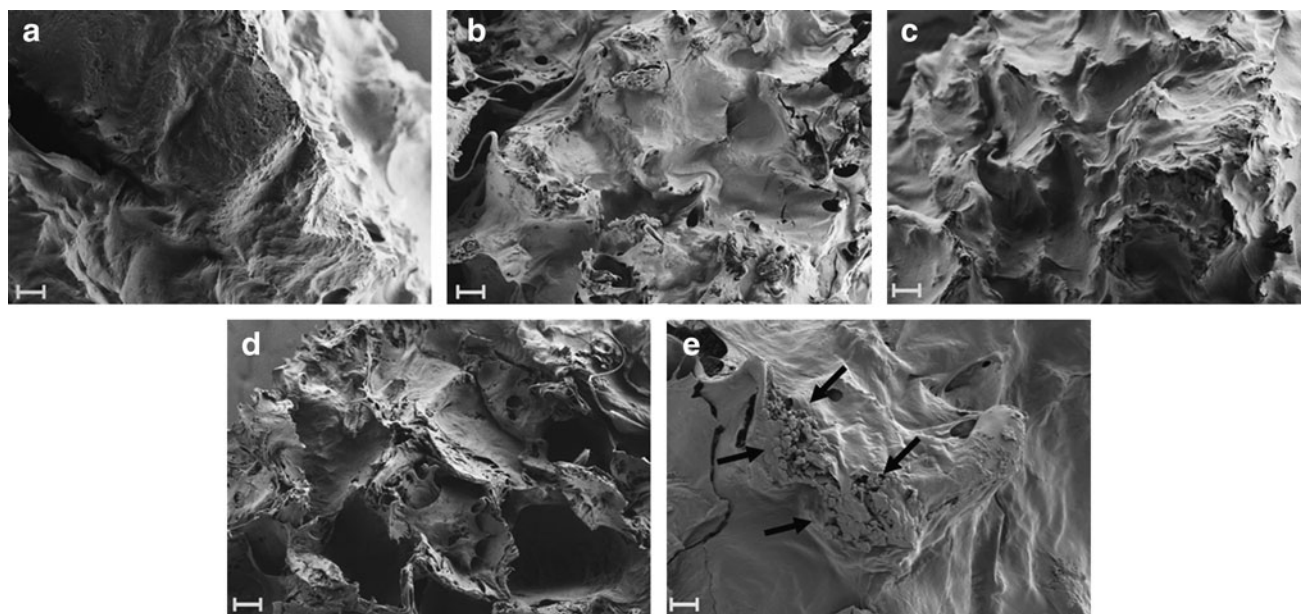


FIG. 1. Scanning electron microscopy images of the different treatment groups cultured with human mesenchymal stem cells at week 7. (a), (b), (c), and (d) shows matrix formation by cells in groups 1 (control), 2 (5 \times lysine and proline), 3 (low oxygen), and 4 (combined effect of low oxygen, 5 \times lysine and proline), respectively, at 200 \times (scale bars = 100 μm). (e) shows the presence of mineralized nodules, marked by black arrows, in group 4 (combined effect of low oxygen, 5 \times lysine and proline) at 600 \times (scale bar = 10 μm).

Model 2475 multi λ fluorescence detector at an excitation of 250 nm and emission of 395 nm (Waters).

Statistical analysis

Statistical differences between each group means were determined by Student-Newman-Keuls *post-hoc* analysis of variance. Statistical significance was assigned as * denoting $p < 0.05$.

Results

Bone matrix formation

All of the treated groups exhibited bone matrix formation, with the cells occupying the interconnected pores (Fig. 1). The SEM images at week 7 (Fig. 1) showed more matrix deposition than at week 2 (Fig. 1, Supplemental Fig. S1, available online at

www.liebertonline.com/ten). The formation of mineralized nodules can be observed in the SEM images of group 4 (combined effect of low oxygen, 5 \times lysine and proline) (Fig. 1e).

Hematoxylin and eosin-stained images showed the presence of cells within the scaffolds in all the groups (Fig. 2). The immunohistochemistry results showed increased mineralization and collagen matrix deposition at week 7 compared to week 2 (data shown in Supplemental Fig. S2, available online at www.liebertonline.com/ten). At week 7, all of the treated groups showed prominent black staining indicative of calcium deposition and brown staining indicative of collagen deposition (Fig. 2).

Biochemical analysis

Figure 3 shows the DNA content of the different groups at weeks 2 and 7 (final culture time). There was no significant

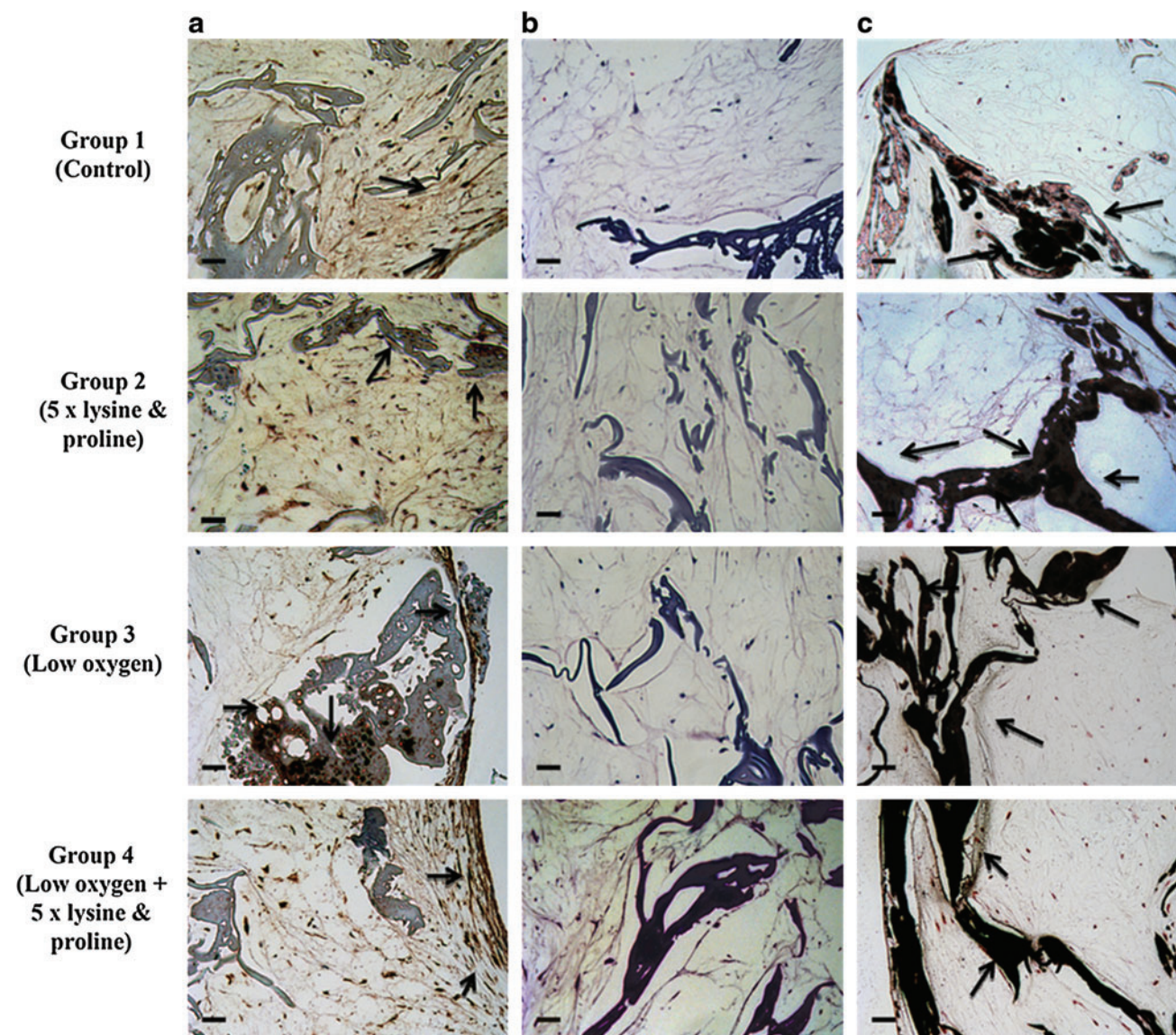


FIG. 2. Images of (a) Coll immunostaining, (b) hematoxylin and eosin staining, and (c) von Kossa staining of the different treatment groups at week 7, under light microscope at 20 \times . All scale bars = 50 μ m. The presence of collagen and calcium is shown by brown and black staining respectively, both of which are marked by black arrows. Coll, collagen type I. Color images available online at www.liebertonline.com/ten.

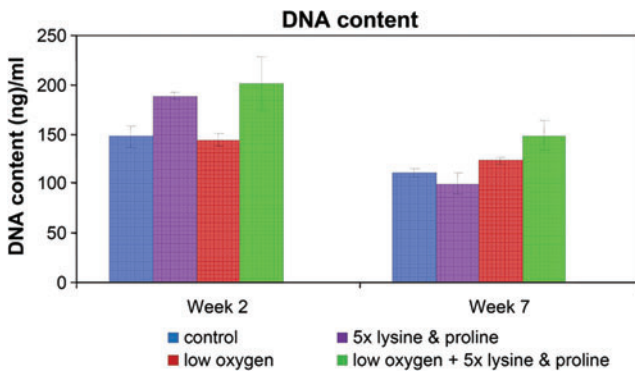


FIG. 3. Picogreen assay was done to assess the DNA content within scaffolds from each group. Color images available online at www.liebertonline.com/ten.

difference in DNA content over time since the cells were cultured in differentiation media and not expected to proliferate. In addition, the DNA content of the cells was not significantly different between the different groups (Fig. 3). ALP,

an early stage marker of osteogenesis, was active in all of the groups at week 2 and decreased in activity at week 7. At week 2, the presence of lysine and proline significantly increased ALP activity in group 2 (5× lysine and proline) compared to group 1 (control). At week 7, group 3 (low oxygen) showed significantly lower ALP activity than group 1 (control). Collagen and calcium content increased over time for all groups, indicating matrix formation and mineralization, respectively. Group 4 (combined effect of low oxygen, 5× lysine and proline) showed a significant increase in collagen and calcium content compared to all other groups (Fig. 4).

Gene expression

Being an early stage osteogenesis marker, the level of *ALP* gene expression was higher in all the groups at week 2 as compared to week 7. At week 2, groups 2 (5× lysine and proline) and 4 (combined effect of low oxygen, 5× lysine and proline) showed significantly higher *ALP* gene expression than group 1 (control). At week 7, both groups 3 (low oxygen) and 4 (combined effect of low oxygen, 5× lysine and proline)

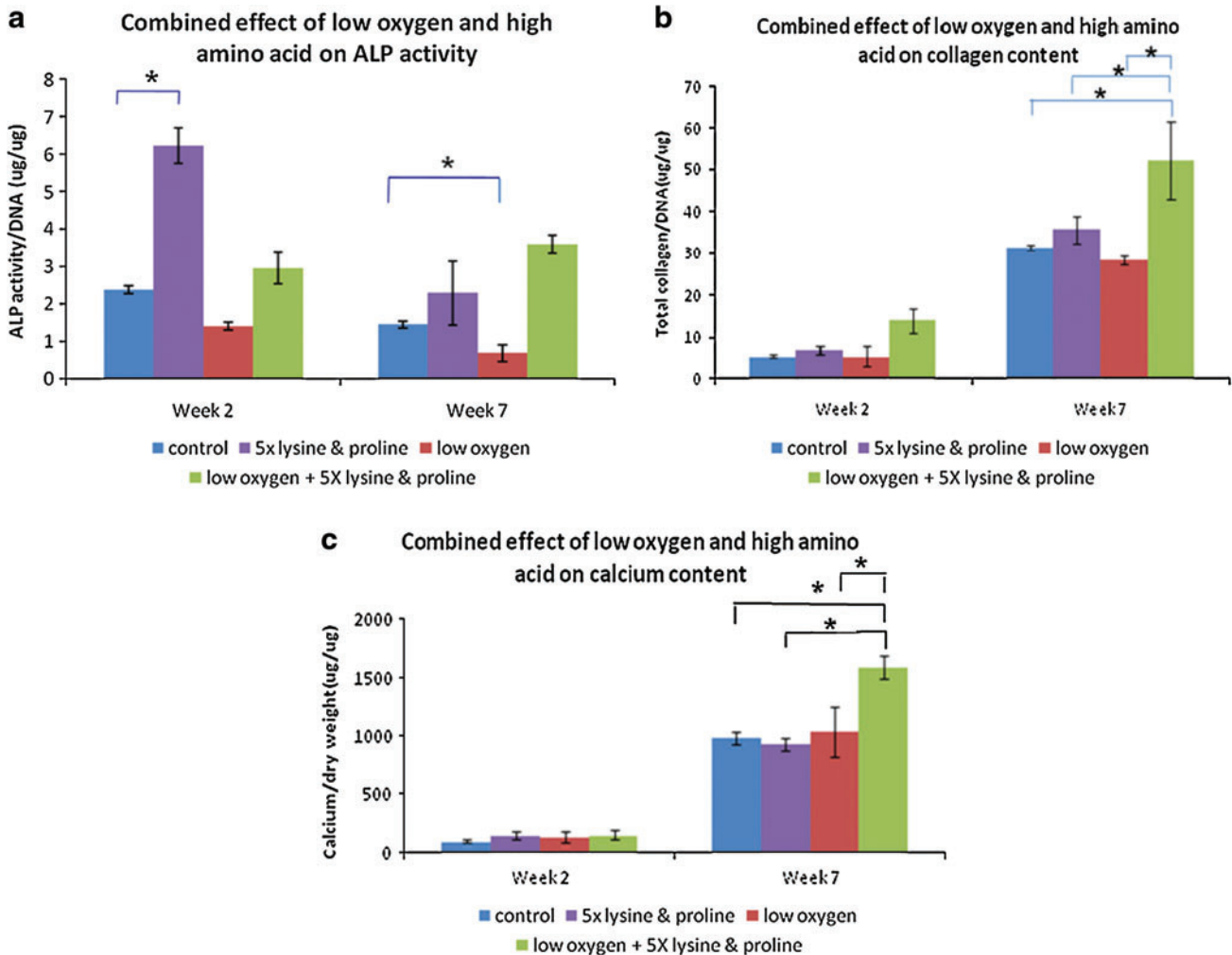


FIG. 4. Chemical analysis tests studied (a) ALP activity, (b) collagen content, and (c) calcium content, which are important indicators of osteogenesis. The figure shows the combined effect of low oxygen and 5× lysine and proline on these osteogenesis outcomes. Statistical significance was assigned as * denoting $p < 0.05$. ALP, alkaline phosphatase. Color images available online at www.liebertonline.com/ten.

showed a significant decrease in *ALP* gene expression when compared to group 1 (control). At week 7, group 2 (5× lysine and proline) exhibited significantly higher *Runx2* gene expression than that of group 1 (control). Group 4 (combined effect of low oxygen, 5× lysine and proline) showed a significant increase in the gene expression levels of *Runx2* and *Collα* as compared to that of when compared to group 1 (control), at week 2 as well as week 7. As compared to group 1 (control), expression of *HIF-1α* gene was significantly elevated in low oxygen conditions in groups 3 (low oxygen) and 4 (combined effect of low oxygen, 5× lysine and proline), both at weeks 2 and 7 (Fig. 5).

Metabolic analysis

The rates of lactate synthesis and glucose consumption were calculated at weeks 2 and 7 and normalized to the DNA content of the scaffolds at the corresponding time point. An increase in metabolic activity was seen with time in all of the groups at week 7 as compared to week 2. A significant increase in lactate synthesis rate was exhibited in group 4 (combined effect of low oxygen 5× lysine and proline) relative to group 1 (control). Glucose consumption was significantly

higher in groups 2 (5× lysine and proline) and 4 (combined effect of low oxygen, 5× lysine and proline) when compared to group 1 (control) (Fig. 6).

In all groups, there was a significant increase in the consumption of the following amino acids: glutamate, glutamine, proline, and lysine at week 7 compared to week 2. Group 2 (5× lysine and proline) showed significantly high lysine consumption as compared to group 1 (control). Group 4 (combined effect of low oxygen, 5× lysine and proline) showed significantly higher consumption of lysine, proline, and glutamate as compared to group 1 (control). Glutamine consumption was significantly lower in groups 3 (low oxygen) and 4 (combined effect of low oxygen, 5× lysine and proline) compared to group 1 (control) (Fig. 7).

Discussion

Each of the different groups showed *in vitro* osteogenesis. Group 2 (5× lysine and proline) caused early upregulation in expression of certain osteogenesis-related genes, such as *ALP* and *Runx2* (Figs. 4 and 5). Although group 3 (low oxygen) decreased the level of *ALP* gene, it did not cause an overall change in osteogenesis. Group 4 (combined effect of low

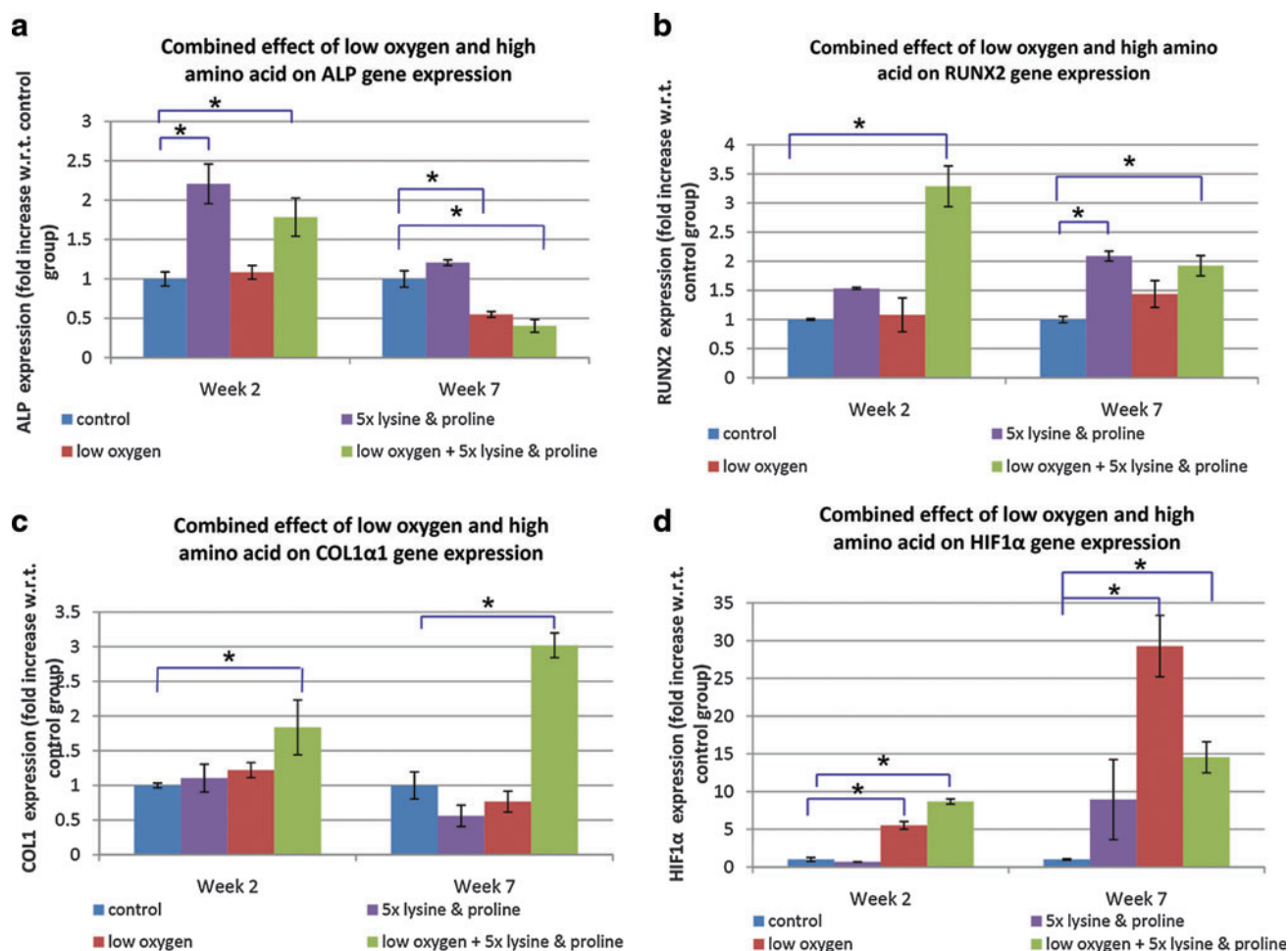


FIG. 5. Semi-quantitative reverse transcriptase polymerase chain reaction measured gene expression of certain bone markers and hypoxia marker. The figure shows the effect of low oxygen and 5× lysine and proline on the gene expression levels of osteogenic markers: (a) *ALP*, (b) *Runx2*, and (c) *Coll*. Expression of the gene (d) *HIF-1α* was also studied to assess the effect of hypoxic condition on gene expression. Statistical significance was assigned as * denoting $p < 0.05$. *HIF*, hypoxia inducible factor; *Runx2*, runt-related transcription factor 2. Color images available online at www.liebertonline.com/ten.

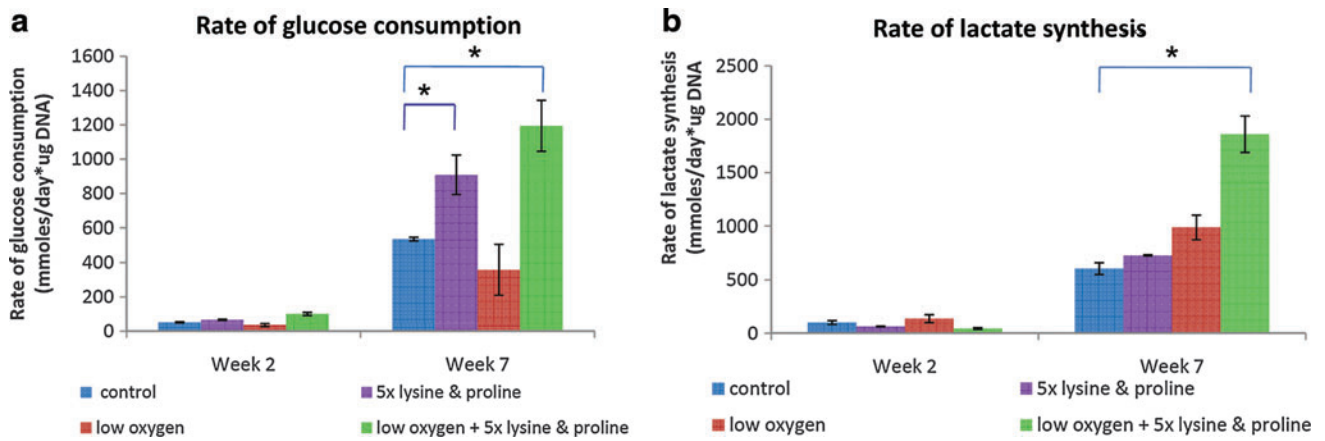


FIG. 6. Analysis of (a) glucose and (b) lactate content of the media demonstrated the effect of low oxygen and high proline and lysine concentration on the metabolic activity of the cells. Statistical significance was assigned as * denoting $p < 0.05$. Color images available online at www.liebertonline.com/ten.

oxygen, 5× lysine and proline) significantly increased osteogenesis, relative to the other groups in almost all aspects (Figs. 4 and 5).

Taken together, the results of our osteogenic and metabolic analyses and known literature suggest the following model of substrate and signaling interactions between osteogenesis

related biosynthetic pathways and intermediary metabolism (Fig. 8). One of the reasons for the significant upregulation in osteogenesis seen in group 4 (combined effect of low oxygen, 5× lysine and proline) is the increased metabolic activity, in terms of both glucose consumption rate and lactate synthesis rate (Fig. 6). In addition, group 4 (combined effect of low

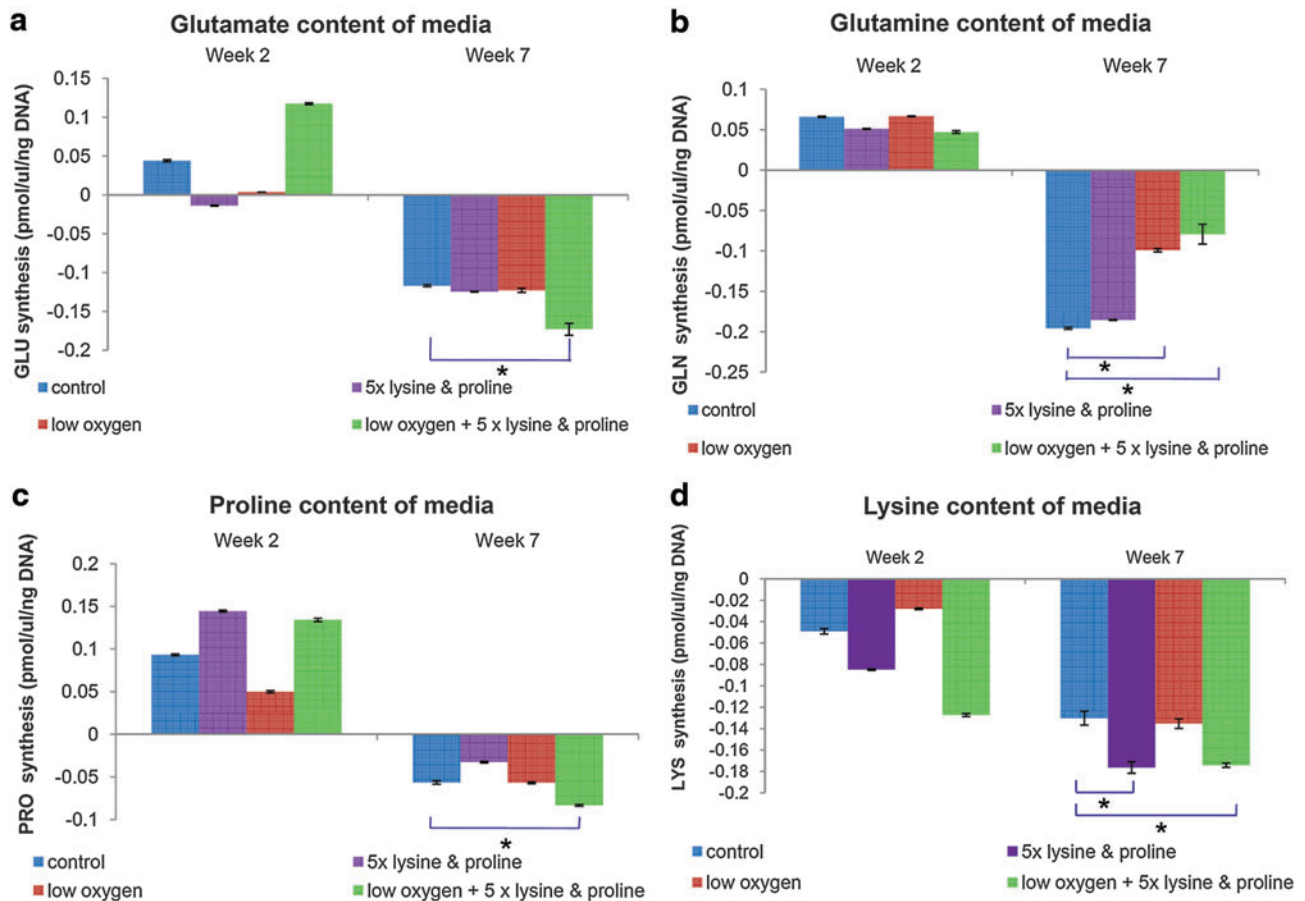


FIG. 7. High performance liquid chromatography results show the consumption of amino acids, (a) glutamate, (b) glutamine, (c) proline, and (d) lysine, during osteogenesis under the effect of low oxygen and high lysine and proline concentration. Statistical significance was assigned as * denoting $p < 0.05$. Color images available online at www.liebertonline.com/ten.

oxygen, 5× lysine and proline) also exhibited increased consumption of the amino acids: lysine, proline, and glutamate (Fig. 7). The increased consumption of lysine and proline residues is believed to be directed toward higher rate of collagen matrix synthesis.^{23,26} While lysine is an essential amino acid, proline is synthesized from glutamate.⁴⁰ Thus, higher consumption of glutamate indicates higher proline biosynthesis. Glutamate is also known to promote osteoblast differentiation and thereby bone formation.⁴¹ However, glutamine consumption was significantly lower under low oxygen conditions in group 3 (low oxygen) and group 4 (combined effect of low oxygen, 5×lysine and proline) (Fig. 7). Glutamine is interconverted to glutamate, which is then taken up in the form of α -keto glutarate in Kreb's cycle during aerobic respiration.⁴⁰ Under limited oxygen availability, aerobic respiration in the form of the Kreb cycle is inhibited,⁴² thus limiting glutamine consumption (Fig. 8).

Our results showed significant upregulation of *HIF-1 α* gene expression in group 3 (low oxygen) and group 4 (combined effect of low oxygen, 5× lysine and proline) (Fig. 5). Reduced intracellular oxygen tension activates *HIF* expression, leading to the subsequent activation of target genes that accelerate bone regeneration.^{29,43} *HIF-1 α* and *HIF-2 α* have been reported

to upregulate expression of an array of angiogenic proteins like erythropoietin and vascular endothelial growth factor.³² *HIFs* have also been known to induce elevated level of glycolytic enzymes like glucose transporter and lactate dehydrogenase enzyme responsible for lactate synthesis postglycolysis. In addition, *HIFs* are believed to promote prolyl hydroxylase enzyme activity, which indirectly promotes collagen matrix synthesis.⁴⁴ However, the study suggested that the upregulation of *HIF-1 α* alone is not sufficient to cause an overall significant increase in osteogenesis and metabolism in group 3 (low oxygen).

The metabolic processes involved in post-translational modification during collagen biosynthesis are one of the major activities influencing bone regeneration. The hydroxylation of proline and lysine residues is an important rate-limiting step in collagen biosynthesis.^{25,45} Thus, the enzymes involved in these reactions, namely, lysyl- and prolyl-hydroxylases, are instrumental in determining the rate of synthesis of fibrillar collagen. However, lysyl and prolyl hydroxylases usually exist in their inactive proenzyme form in mammalian tissues.⁴⁶ As a result, lysine and proline hydroxylation and thereby collagen synthesis are inhibited. This may explain why amino acid supplementations did not

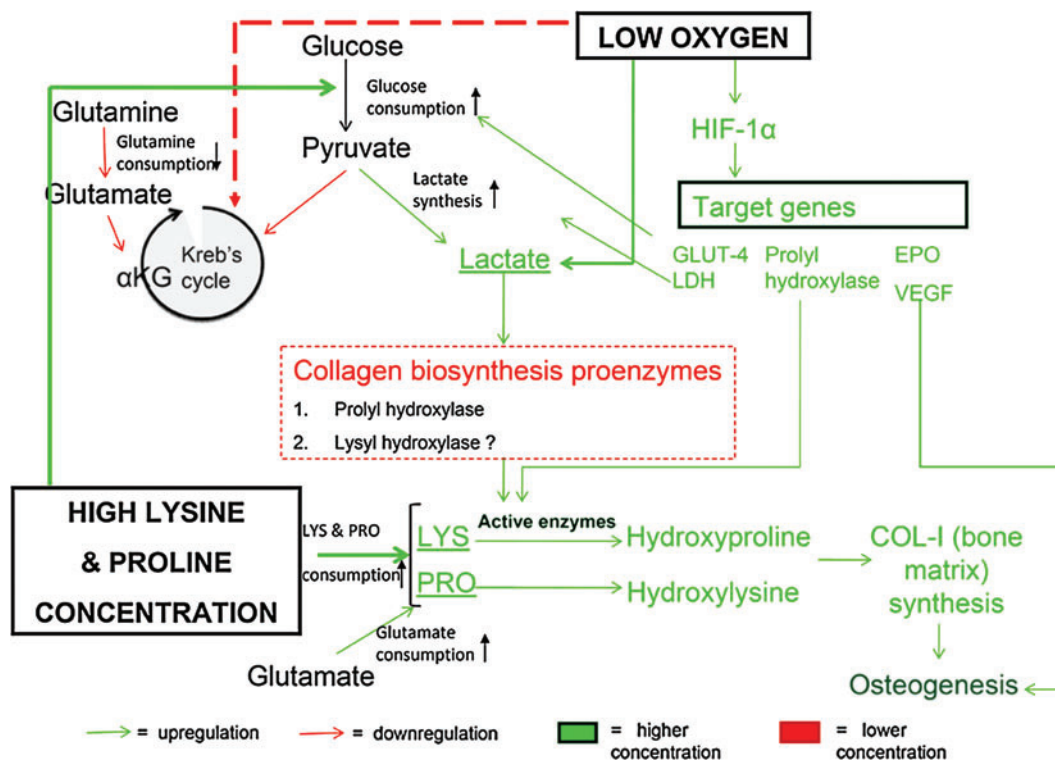


FIG. 8. On the basis of the results of this study and known pathways relating energy metabolism and matrix metabolism, the given metabolic model flowchart was derived. It describes the mechanism behind increased osteogenesis rate in the presence of low oxygen as well as high proline and lysine concentration. Low oxygen triggers expression of *HIF-1 α* , which in turn upregulates expression of a number of target genes that directly or indirectly help in osteogenesis. The glucose consumption rate as well as lactate synthesis rate increases in the presence of low oxygen, while *Kreb's* cycle and thereby glutamine consumption is downregulated. Lactate accumulation, in turn, has been reported to activate prolyl hydroxylase proenzyme. This enzyme catalyses hydroxylation of proline residues and thus plays an important role in collagen biosynthesis. High lysine and proline concentration increases lysine and proline consumption and thereby increases glutamate consumption, the net result being an upregulation in collagen synthesis and bone formation. Color images available online at www.liebertonline.com/ten.

significantly enhance collagen deposition and thereby osteogenesis in group 2 (5× lysine and proline).

In summary, based on our findings and known literature, it is speculated that the stimulatory effect of amino acid supplementation and low oxygen treatment are due to the following sequences of metabolic and signaling events. Low oxygen triggers expression of *HIF-1 α* (Fig. 6A), which elevates the level of glycolytic enzymes, collagen matrix synthesis enzymes, and angiogenic factors to enhance osteogenesis.^{29–31,43,44} Due to the increased glycolytic rate, there is an increase in the rate of glucose consumption (Fig. 6). The end product of glycolysis, pyruvic acid, is reduced to lactate under low oxygen conditions,³⁹ which leads to the observed increase in lactate synthesis (Fig. 6). Lactate accumulation signals the metabolic need to stabilize *HIF* expression and regulate redox balance, thus facilitating more glycolysis, collagen deposition, and angiogenesis in a positive feedback loop.^{47,48} Moreover, it was seen in rat and mouse fibrillar collagen that supplying lactate to the culture activates prolyl hydroxylase proenzyme by suppressing ADP-ribosylation.^{46,49,50} Increased lactate production thus induces hydroxylation of proline. Past literature and our results suggest that an increase in lactate concentration might also activate lysine hydroxylase proenzyme leading to increased lysine consumption.⁴⁶ High concentration of lysine and proline in the amino acid supplemented media ensures that a higher number of lysine and proline residues are hydroxylated by the activated enzymes and utilized for collagen matrix assembly. This explains the increased collagen protein deposition observed in Figures 2 and 3. However, this does not fully explain why *Col1 α 1* gene expression was elevated in the presence of the combined effect of low oxygen and high lysine and proline concentrations (Fig. 4). The net result is a significantly higher osteogenesis rate under the combined effect of low oxygen and high lysine and proline concentration (group 4) when compared to control (group 1) or either of the effects alone (group 2 or group 3) (Figs. 4 and 5).

In future, the proposed metabolic model (Fig. 8) can be tested by altering specific gene expression(s) or metabolite concentration(s) to assess their individual effect on osteogenesis. For example, knockdown or overexpression of *HIF-1 α* and/or its target genes will confirm their effect on osteogenic outcomes. Also, the implication of lactate as a crucial intermediate factor regulating collagen biosynthesis can be confirmed by the addition or removal of lactate from the media and monitoring the corresponding changes in enzyme (lysine and proline hydroxylase) concentration and osteogenic rates.

Conclusions

The combined effect of low (5%) oxygen and high lysine and proline concentration (group 4) significantly enhanced osteogenesis rate of hMSCs on silk protein scaffolds, when compared to the control (group 1) or either of the conditions alone (group 2 or group 3) *in vitro*. This outcome was in part due to alterations in the metabolic response of the differentiating human mesenchymal cells. Metabolic activity in terms of glucose consumption rate, lactate synthesis rate, and utilization of the amino acids lysine, proline, glutamate, and glutamine had profound implications on osteogenesis rates.

Thus, a link between metabolism and osteogenesis from hMSCs *in vitro* was found. In addition to elucidating the impact of low oxygen and amino acid supplementations on osteogenesis and postulating an underlying metabolic pathway, the findings of this study provide a starting point for matching tissue engineering strategies to specific osteogenesis needs. The osteogenic response of the cells for the chosen set of input parameters and corresponding metabolic demands will be used for building a predictive model for osteogenesis rates. On the basis of metabolic profiles for a patient, as well as conditions at a defect site, the model will enable us to predict desired rates of osteogenesis for designing personalized bone implants in the future. Other factors like hMSC sources and scaffold features will also be considered in the model for predicting their influence on osteogenesis.

Acknowledgments

We appreciate the technical contributions by Carmen Preda. This work was supported by NIH P41 Tissue Engineering Resource Center (P41 EB002520).

Disclosure Statement

No competing financial interests exist.

References

1. Franceschi, R.T. Biological approaches to bone regeneration by gene therapy. *J Dent Res* **84**, 1093, 2005.
2. Khanzada, R.N., Holy, C.E., Volenec, J., and Bruder, S.P. Cell therapies for bone regeneration. In: Atala, A., Lanza, R., Thomson, J., and Nerem, R., eds. *Principles of Regenerative Medicine*. Burlington, MA: Elsevier Science & Technology, 2008, pp. 868–884.
3. Mistry, A.S., and Mikos, A.G. *Tissue Engineering Strategies for Bone Regeneration*. *Regenerative Medicine II*, Vol. 94. New York: Springer Berlin/Heidelberg, 2005, pp. 1–22.
4. Pietrzak, W.S. *Musculoskeletal Tissue Regeneration: Biological Materials and Methods*, Vol. 11. New Jersey: Humana Press, 2008.
5. Guldberg, R.E., and Duty, A.O. Design parameters for engineering bone regeneration. In: Guilak, F., Butler, D.L., Goldstein, S.A., and Mooney, D., eds. *Functional Tissue Engineering*. New York: Springer-Verlag, 2003, pp. 146–161.
6. Kim, H.J., Kim, U., Vunjak-Novakovic, G., Min, B., and Kaplan, D.L. Influence of macroporous protein scaffolds on bone tissue engineering from bone marrow stem cells. *Biomaterials* **26**, 4442, 2005.
7. Meinel, L., Fajardo, R., Hofmann, S., Langer, R., Chen, J., Snyder, B., *et al.* Silk implants for the healing of critical size bone defects. *Bone* **37**, 688, 2005.
8. Wang, Y., Kim, H., Vunjak-Novakovic, G., and Kaplan, D.L. Stem cell-based tissue engineering with silk biomaterials. *Biomaterials* **27**, 6064, 2006.
9. Akintoye, S.O., Lam, T., Shi, S., Brahim, J., Collins, M.T., and Robey, P.G. Skeletal site-specific characterization of orofacial and iliac crest human bone marrow stromal cells in same individuals. *Bone* **38**, 758, 2006.
10. Sanz-Herrera, J.A., García-Aznar, J.M., and Doblaré, M. On scaffold designing for bone regeneration: a computational multiscale approach. *Acta Biomater* **5**, 219, 2009.

11. Kim, U., Park, J., Joo Kim, H., Wada, M., and Kaplan, D.L. Three-dimensional aqueous-derived biomaterial scaffolds from silk fibroin. *Biomaterials* **26**, 2775, 2005.
12. Hofmann, S., Hagenmüller, H., Koch, A.M., Müller, R., Vunjak-Novakovic, G., Kaplan, D.L., *et al.* Control of *in vitro* tissue-engineered bone-like structures using human mesenchymal stem cells and porous silk scaffolds. *Biomaterials* **28**, 1152, 2007.
13. Rechenberg, B.V., Uebersax, L., Apfel, T., Schubotz, R., Hilbe, M., Meinel, L., Kim, H.J., Kaplan, D.L., Merkle, H.P., and Auer, J.A. Silk fibroin as an adaptable 3-D scaffold for defect repair in subchondral bone. *Eur Cells Mater* **13**, 15, 2007.
14. Uebersax, L., Hagenmüller, H., Hofmann, S., Gruenblatt, E., Müller, R., Vunjak-Novakovic, G., Kaplan, D.L., Merkle, H.P., and Meinel, L. Effect of scaffold design on bone morphology *in vitro*. *Tissue Eng* **12**, 3417, 2006.
15. Hao, L., and Harris, R. Customised Implants for Bone Replacement and Growth. In: Bartolo, P., and Bidanda, B., eds. *Bio-Materials and Prototyping Applications in Medicine*. New York: Springer, 2008, pp. 79–107.
16. Fernández-Tresguerres-Hernández-Gil, I., Alobera-Gracia, M.A., del Canto-Pingarrón, M., and Blanco-Jerez, L. Physiological bases of bone regeneration II. The remodeling process. *Med Oral Patol Oral Cir Bucal* **11**, E151, 2006.
17. Djouad, F., Delorme, B., Maurice, M., Bony, C., Apparailly, F., Louis-Pence, P., *et al.* Microenvironmental changes during differentiation of mesenchymal stem cells towards chondrocytes. *Arthritis Res Ther* **9**, R33, 2007.
18. Jaiswal, N., Haynesworth, S., Caplan, A., and Bruder, S. Osteogenic differentiation of purified, culture-expanded human mesenchymal stem cells *in vitro*. *J Cell Biochem* **64**, 295, 1997.
19. Benoit, D.S.W., Schwartz, M.P., Durney, A.R., and Anseth, K.S. Small functional groups for controlled differentiation of hydrogel-encapsulated human mesenchymal stem cells. *Nat Mater* **7**, 816, 2008.
20. Follmar, K.E., DeCroos, F.C., Prichard, H.L., Wang, H.T., Erdmann, D., and Olbrich, K.C. Effects of glutamine, glucose, and oxygen concentration on the metabolism and proliferation of rabbit adipose-derived stem cells. *Tissue Eng* **12**, 3525, 2006.
21. Blaine, M.T., Keith, F.E., Kurtis, M.E., Ben, B., Kevin, O.C., Scott, L.L., Bruce, K., and Detlev, E. Metabolic and functional characterization of human adipose-derived stem cells in tissue engineering. *Plast Reconstr Surg* **122**, 725, 2008.
22. Park, S.H., Gil, E.S., Shai, H., Kim, H.J., Lee, K., and Kaplan, D.L. Relationships between degradability of silk scaffolds and osteogenesis. *Biomaterials* **31**, 6162, 2010.
23. Moreira, P.L., An, Y.H., Santos, A.R., and Genari, S.C. *In vitro* analysis of anionic collagen scaffolds for bone repair. *J Biomed Mater Res Part B Appl Biomater* **71B**, 229, 2004.
24. Young, M.F. Bone matrix proteins: more than markers. *Calcif Tissue Int* **72**, 2, 2003.
25. Diegelmann, R.F. Collagen Metabolism. *Wounds* **13**, 2002. Available at www.medscape.com/viewarticle/423231.
26. Shoulders, M.D., and Raines, R.T. Collagen structure and stability. *Annu Rev Biochem* **78**, 929, 2009.
27. Tsuji, N., Shimomura, Y., Yabuuchi, Y., Hayashi, H., and Ohgushi, H. Osteogenic influence of lysine in porous hydroxyapatite scaffold. *Key Eng Mater* **361**, 1189, 2008.
28. Lu, C., Rollins, M., Hou, H., Swartz, H.M., Hopf, H., Mclau, T., and Marcucio, R.S. Tibial fracture decreases oxygen levels at the site of injury. *Iowa Orthop J* **28**, 14, 2008.
29. Wan, C., Gilbert, S.R., Wang, Y., Cao, X., Shen, X., Ramaswamy, G., *et al.* Activation of the hypoxia-inducible factor-1 α pathway accelerates bone regeneration. *Proc Natl Acad Sci USA* **105**, 686, 2008.
30. Wang, Y., Wan, C., Gilbert, S.R., and Clemens, T.L. Oxygen sensing and osteogenesis. *Ann NY Acad Sci* **1117**, 1, 2007.
31. Wang, Y., Wan, C., Deng, L., Liu, X., Cao, X., Gilbert, S.R., *et al.* The hypoxia-inducible factor α pathway couples angiogenesis to osteogenesis during skeletal development. *J Clin Invest* **117**, 1616, 2007.
32. Potier, E., Ferreira, E., Andriamanalijaona, R., Pujol, J.-P., Oudina, K., Logeart-Avramoglou, D., *et al.* Hypoxia affects mesenchymal stromal cell osteogenic differentiation and angiogenic factor expression. *Bone* **40**, 1078, 2007.
33. Utting, J.C., Robins, S.P., Brandao-Burch, A., Orriss, I.R., Behar, J., and Arnett, T.R. Hypoxia inhibits the growth, differentiation and bone-forming capacity of rat osteoblasts. *Exp Cell Res* **312**, 1693, 2006.
34. Osipenko, A., and Makarova, E. Energy metabolism in lymphocytes during bone tissue regeneration. *Bull Exp Biol Med* **120**, 949, 1995.
35. Khomullo, G.V. Regeneration of bone at various metabolic rates. *Bull Exp Biol Med* **53**, 211, 1962.
36. Altman, G.H., Lu, H.H., Horan, R.L., Calabro, T., Ryder, D., Kaplan, D.L., *et al.* Advanced bioreactor with controlled application of multi-dimensional strain for tissue engineering. *J Biomech Eng* **124**, 742, 2002.
37. Trinder, P. Determination of blood glucose using an oxidase-peroxidase system with a non-carcinogenic chromogen. *J Clin Pathol* **22**, 158, 1969.
38. Cohen, S.A., and De Antonis, K.M. Applications of amino acid derivatization with 6-aminoquinolyl-N-hydroxysuccinimidyl carbamate: analysis of feed grains, intravenous solutions and glycoproteins. *J chromatogr* **661**, 25, 1994.
39. Cohen, S.A. Amino acid analysis using precolumn derivatization with 6-aminoquinolyl-n-hydroxysuccinimidyl carbamate. In: Cooper, C., Packer, N., and Williams, K., eds. *Amino Acid Analysis Protocols*, Vol. 159. Milford, MA: Humana Press, 2000, pp. 39–47.
40. Berg, J.M., Tymoczko, J.L., and Stryer, L. The Biosynthesis of Amino acids. *Biochemistry*. New York: W.H. Freeman, 2002, pp. 665–692.
41. Mason, D.J. Glutamate signalling and its potential application to tissue engineering of bone. *Eur Cells Mater* **7**, 12, 2004.
42. Biological Sciences Curriculum Studies. *The Human Animal: Food and Energy*. BSCS Biology: An Ecological Approach. MA: Kendall/Hunt Publishing Company, 2002, pp. 391–418.
43. Zhu, H., and Bunn, H.F. Signal transduction: how do cells sense oxygen? *Science* **292**, 449, 2001.
44. Koukourakis, M.I., Pitiakoudis, M., Giatromanolaki, A., Tsarouha, A., Polychronidis, A., Sivridis, E., *et al.* Oxygen and glucose consumption in gastrointestinal adenocarcinomas: correlation with markers of hypoxia, acidity and anaerobic glycolysis. *Cancer Sci* **97**, 1056, 2006.
45. Myllylä, R., Wang, C., Heikkinen, J., Juffer, A., Lampela, O., Risteli, M., *et al.* Expanding the lysyl hydroxylase toolbox: New insights into the localization and activities of lysyl hydroxylase 3 (LH3). *J Cell Physiol* **212**, 323, 2007.
46. Risteli, J., and Kivirikko, K.I. Activities of prolyl hydroxylase, lysyl hydroxylase, collagen galactosyltransferase and collagen glucosyltransferase in the liver of rats with hepatic injury. *Biochem J* **144**, 115, 1974.
47. Hunt, T.K., Aslam, R., Hussain, Z., and Beckert, S. Lactate, with oxygen, incites angiogenesis. In: Kang, K.A., Harrison,

- D.K., and Bruley, D.K., eds. *Oxygen Transport to Tissue XXIX*. New York: Springer, 2008, pp. 73–80.
48. Hunt, T.K., Gimbel, M., and Sen, C.K. Revascularization of wounds: the oxygen-hypoxia paradox. In: Figg, W.D., and Folkman, J., eds. *Angiogenesis: An integrative approach from science to medicine*. New York: Springer, 2008, pp. 541–559.
49. Stassen, F.L.H., Cardinale, G.J., McGee, J.O., and Udenfriend, S. Prolyl hydroxylase and an immunologically related protein in mammalian tissues. *Arch Biochem Biophys* **160**, 340, 1974.
50. Hussain, M., Ghani, Q., and Hunt, T. Inhibition of prolyl hydroxylase by poly(ADP-ribose) and phosphoribosyl-AMP. Possible role of ADP-ribosylation in intracellular prolyl hydroxylase regulation. *J Biol Chem* **264**, 7850, 1989.

Address correspondence to:

David L. Kaplan, Ph.D.

Department of Biomedical Engineering

School of Engineering

Tufts University

4 Colby St.

Medford, MA 02155

E-mail: david.kaplan@tufts.edu

Received: May 21, 2010

Accepted: July 8, 2010

Online Publication Date: August 30, 2010